An experimental approach to study multi-species interactions implicated in Fusarium-Head Blight complex assembly in wheat.

2025_04_14

Miguel Ángel Corrales Gutiérrez[1], Harleen Kaur[1], Francesca Desiderio[2], Dimitar Kostadinov Douchkov[3], Jiasui Zhan[1], Heriberto Vélëz[1,4,*], Salim Bourras[5*].

Authors affiliation

[1]. Department of Forest Mycology and Plant Pathology, Swedish University of Agricultural Sciences. Almas Allé 5, 75007 Uppsala, Sweden.

[2]. Council for Agricultural Research and Economics (CREA) - Research Centre for Genomics and Bioinformatics, Fiorenzuola d'Arda, Italy

[3]. Leibniz-Institute of Plant Genetics and Crop Plant Research, 06466-Gatersleben, Germany.

[4]. Current address: College of Science, Mathematics and Technology. Wenzhou-Kean University. 88 Daxue Rd, Ouhai, Wenzhou, Zhejiang Province 325060, China.

[5]. Department of Plant Biology, Swedish University of Agricultural Sciences. Almas Allé 5, 75007 Uppsala, Sweden.

Authors for correspondence

Dr. Heriberto Vélëz

hvelez@kean.edu

Prof. Dr. Salim Bourras

salim.bourras@slu.se

Abstract

Fusarium Head Blight (FHB) is a major disease of cereal crops present everywhere where wheat is produced. A complex of several, distinctly different, species from the genus *Fusarium* are responsible for causing the disease, with important taxa being *F. graminearum*, *F. culmorum*, and *F. avenaceum*. FHB is an adult stage, late season disease affecting wheat at anthesis. However, recent discoveries are now challenging the basic assumption that anthers and spikes are the only ecological niches relevant for resistance to FHB. Most prominently, it has been established that pathogens typically occurring earlier in the season, such as *Zymoseptoria tritici*, induce strong systemic changes in the plant immune system, that expand way beyond their primary ecological niche. Furthermore, taxa implicated in FHB can be isolated from virtually all wheat tissues, including typical blotch symptoms on wheat leaves. Strikingly, such important biological observations about the complex lifestyle of FHB causing taxa are overlooked as potential targets in resistance breeding. In this work we present a simplified approach allowing the dissection of the intricate lifestyles of the FHB causing *Fusarium* taxa. In doing so, we provide an experimental proof-of-concept that systemic signals from *Z. tritici* can affect the basic response of wheat to *F. graminearum*. We further demonstrate that differences in *Fusarium* species composition affect the outcome of the interaction in a genotype-specific manner. We argue that efforts to study hidden layers of the biology of FHB associated taxa are crucial to developing new resistance breeding strategies, based on a better understanding of the genetic drivers of the disease.

Introduction

Fusarium Head Blight (FHB) is a wheat disease caused by a multispecies complex of up to 17 distinctly different *Fusarium* and non-*Fusarium* taxa (Karlsson *et al*., 2021). In nature, *Fusarium* ssp. are ubiquitous colonizers of monocot grasses that can be found in all tissues from roots to seeds. This is consistent with the piling evidence suggesting that pathogenic *Fusarium* taxa have evolved from endophytic *Fusarium* species, including those implicated in FHB (Hill *et al*., 2022; Ma *et al*., 2013). Despite this evolutionary trajectory, the *Fusarium* genomes have no clear signatures of lifestyle transition, even though such events are frequent in *Fusarium* fungi (Hill *et al*., 2022). This is strikingly contrasting with other ubiquitous colonizers such as Hypocreales fungi, where comparative genomic studies have revealed clear, lifestyle specific, genetic signature underlying the ability of these fungi to inhabit different hosts and environments (Wu & Cox, 2021). This suggests that lifestyle requirements in *Fusarium* fungi are very plastic, which is indeed the case with those associated with FHB. For instance, *F. graminearum* can survive as a saprophyte on wheat debris, while the most common pathogenic taxa implicated in FHB including *F. graminearum*, *F. culmorum*, and *F. avenaceum* can be found as latent endophyte inhabiting wheat stems, leaves, and roots (Kaur & Vilvert, *et al*., 2024; Lidia *et al*., 2021). Furthermore, it was also shown that FHB associated taxa can cause blotch-like symptoms on wheat leaves thus demonstrating that lifestyles shifts can occur in tissues where *Fusarium* spp. are present as silent endophytic colonizers (Kaur & Vilvert, *et al*., 2024).

Altogether, these data indicate that FHB causing taxa are present in the wheat host, very early in the season, throughout development, prior to anthesis. This is major because the etiology of FHB is often assimilated to the biology of *F. graminearum* with a two-step process is initiated at anthesis by for instance airborne spores landing in the anthers, which further spread through the rachis. Several studies have addressed the relative predominance of the different taxa implicated in FHB in relation to years and/or location. In Australia, several FHB epidemics in the 1980s, 1990s, and 2000s were incited by *F. pseudograminearum* (Burgess *et al*., 1987; Obanor *et al*., 2013; Obanor & Chakraborty, 2014). This is striking, because *F. pseudograminearum* is mostly associated with a disease called Fusarium Crown Rot, which affects a distinctly different wheat tissue at a much earlier developmental stage (Kazan & Gardiner, 2018). Thus, there can be large variations in complex composition, including several cases where *F. graminearum* was not the most prevalent species (Doohan *et al*., 2003; Lukanowski *et al*., 2008; Parry *et al*., 1995; Waalwijk *et al*., 2003; Xu *et al*., 2005). For

instance, a field study evaluated the percentage of FHB infected wheat ears colonised by *F. graminearum*, *F. culmorum*, *F. avenaceum*, *F. poae*, and *M. nivale* in seven location throughout east and west Flanders in Belgium (Audenaert *et al*., 2009). The authors found large variation in complex composition across wheat genotypes and environments, with several cases where *F. poae* was the most predominant species causing FHB (Audenaert *et al*., 2009). In Italy, a large population study showed large shifts in FHB complex composition where *F. graminearum* was replaced by *F. poae* as the main taxon, and even supplanted by *M. Nivale* and *F. verticillioides* (Valverde-Bogantes *et al*., 2020). Finally in Kenya, a field survey where the incidence and severity of FHB were assessed at the hard dough stage showed that *F. avenaceum*, *F. poae* and *F. tricinctum* were the most abundant taxa. In one case. *F. graminearum* was the lowest in abundance of all isolated taxa (Maina *et al*., 2016) .

This again demonstrates the ecological plasticity of FHB associated taxa, further highlighting the importance of lifestyle transition as a potential driver of FHB, and strengthening the argument that resistance to this disease cannot be reduced to *F. graminearum*. It also challenges to genetic assumptions restricting the definition of resistance to FHB to resistance to initial infection (Type I), resistance to the spread of the fungus through the rachis (Type II), resistance to toxin accumulation or the ability to degrade the mycotoxins (Type III), resistance to kernel infection (Type IV), and finally tolerance to yield loss (Type V). Strikingly, all types are restricted to flower/spike as the only tissue relevant to resistance, and all except 'Type IV' have a strong developmental stage-dependent, structural component. Furthermore, 'Type IV' is strongly challenged by recurrent and repeated observations that associations between mycotoxin production and FHB severity are inconsistent, which is a reasonable expectation considering piling evidence that *Fusarium* mycotoxins as antimicrobial compounds primarily directed against other microbes (i.e. not the host) (Sweany *et al*., 2022). Furthermore, *Fusarium* mycotoxin production in wheat is possibly a reminiscence of ancient association with grasses (i.e. the wild ancestors of cereals) where such compounds provide protection against herbivores (Gerling *et al*., 2023). Indeed, wild grasses serve as reservoir for *Fusarium* infections and mycotoxin contamination of wheat, which pinpoints the importance of understanding the endophytic lifestyle and its plasticity among members of the FHB species complex (Gerling *et al*., 2023).

Thus, the very genetic models serving as a basis for resistance breeding fail at accounting for such complexity, and the interplay between different members of the FHB complex. Similarly,

115 such models also overlook important findings highlighting the importance of pathogen-induced
116 systemic signals to wheat immunity (Seybold *et al*., 2020). It has been shown that infection
117 with the foliar wheat pathogen *Zymospetoria tritici* induces systemic and long-lasting
118 immunosuppression in the host (Seybold *et al*., 2020). Such effect was observed in distant
119 organs and tissues that were not infected by *Z. tritici*, thus suggesting that early-stage infection
120 of wheat with foliar pathogens can alter the response to disease occurring later in the season
121 with the most prominent example being FHB. Another striking observation challenging the
122 resistance 'Type' nomenclature, is that none of the 556 QTL identified in wheat as conferring
123 resistance to FHB correspond to a major locus with dominant effect (Steiner *et al*., 2017;
124 Venske *et al*., 2019). Furthermore, not a single immune receptor has been shown to control any
125 form of resistance to FHB (Steiner *et al*., 2017; Venske *et al*., 2019). This is striking
126 considering that the exceptional ability of *Fusarium* spp. to colonize a variety of tissues as
127 silent apoplectic endophytes, which requires initial and permanent suppression of pattern
128 recognition receptors (PRRs) (Saijo *et al*., 2018; Stotz *et al*., 2014). Indeed, the *Fusarium*
129 genomes encode effector proteins, which is a class of fungal factor commonly associated with
130 the suppression of plant immunity in fungal pathogens and non-pathogenic fungal endophytes
131 (Collinge *et al*., 2022; Redkar *et al*., 2022; Rovenich *et al*., 2014). Furthermore, prominent
132 members of the FHB complex such as *F. graminearum*, and *F. culmorum* behave as typical
133 hemibiotrophs in leaf infection assays, with an initial latent, asymptomatic biotrophic phase
134 followed by necrosis induction (Diamond & Cooke, 1999; Kaur & Vilvert, *et al*., 2024).
135
136 Thus, the basic expectation is that the wheat immune response to FHB should involve some
137 form of receptor-ligand interaction implicating well defined host immune receptors. However,
138 the ability to genetically explore such hypothesis is largely restricted by the phenotyping
139 strategies used to score FHB, which are largely aligned to the pre-defined resistance types I to
140 V. Most prominently, interactions between FHB causing taxa and the host are almost
141 exclusively assessed from anthesis onwards, with a large focus on scoring blight symptoms on
142 the spikes and mycotoxin accumulation in the grain (Alisaac & Mahlein, 2023; Khan *et al*.,
143 2020; Mesterhazy, 2020). Still, several alternative phenotyping strategies have been developed
144 to allow large phenotypic screens of more complex traits that cannot be implemented in the
145 field. These include detached leaf assays (Diamond & Cooke, 1999), seedling resistance assays
146 (Mesterhazy, 1987), seed germination assay (Browne & Cooke, 2005), and coleoptile infection
147 assay (Wu *et al*., 2005). Strikingly, while none of these strategies is targeting anthesis, all have
148 proven useful for the identification of resistance traits against FHB in wheat and other cereals.

149 Most prominently, and of direct relevance to this work, assays based on artificial infections of
150 detached leaf assay has been particularly used due to the high correlation between pathogen
151 latent period and quantitative disease resistance in the field (Diamond & Cooke, 1999; Niks &
152 Skinnes, 1998).
153
154 In this work we present a phenotyping strategy designed to investigate the host genetic factors
155 affecting the endophytic lifestyle of *Fusarium* taxa associated with FHB and their ability to
156 associate in a complex. We developed a fully featured phenotyping strategy based on highly
157 controlled detached leaves infections, combined with machine-learning aided image analysis
158 allowing accurate quantification of disease symptoms. In doing so, we also produce an
159 experimental proof-of-concept for the potential role of systemic signals and the host genetic
160 background in controlling lifestyle transition and complex assembly, thus providing a working
161 system for mining potentially novel FHB resistance traits.
162
163 **Methods**
164 **Plant growth conditions.**
165 An overview of the phenotyping pipeline is provided in **Figure 1**. In this study, we used the
166 reference hexaploid wheat cultivars Chinese Spring, Fielder, and Bob-white; the breeding lines
167 Agadir, Artico, and Victo which are *Triticum aestivum* spp. *aestivum*; Latino, a *T. turgidum* spp.
168 *durum* cultivar, MG5323, a *T. dicoccum* accession, and Zardak, an old cultivar of *T. turgidum*
169 spp. *turanicum*. We also used 30 commercial spring wheat cultivars commonly grown in
170 Sweden provided by the Swedish Agricultural Cooperative Lantmännen Lantbruk (Sweden).
171 All genotypes were germinated in pots with sterilized substrate at 20-21 °C, RH of 70% and
172 with light intensity of 300 µmol and 18 h light/ 6 h dark photoperiod. Plants for inoculation
173 with *Z. tritici* were maintained in a closed infection chamber inside a growth chamber with the
174 same above conditions, and supplemented with additional LED light sources enriching the light
175 spectrum in the 380 and 700 nM wavelength, respectively (**Supplementary Figure 1**).
176
177 **Preparation of *Zymoseptoria tritici* inoculum**
178 *Z. tritici* isolates ST99CH_3B8 (abbreviated as 3B8), ST99CH_3C4 (3C4), ST99CH_3C7
179 (3C7), ST99CH_3D5 (3D5), ST99CH_3D7 (3D7), ST99CH_3F2 (3F2), ST99CH_3G6 (3G6)
180 were isolated in Switzerland in 1999 (courtesy of Prof. Bruce McDonald, Federal Institute of
181 Technology, ETH Zürich, Switzerland). *Z. tritici* isolates were incubated in yeast extract-malt
182 extract-starch agar medium (YMS 4 g/L yeast extract, 4 g/L malt extract, 4 g/L sucrose, 16 g/L

183 agar), in darkness at 20 °C for 11 days until the day of the infection. Spores were collected
184 from the plates by scraping the cells in sterile conditions and resuspend in TWEEN 0.01%. The
185 solution was filtered with a cloth with pore diameter of 22-25 µm. Spore concentration was
186 determined with a hemocytometer and adjusted in all isolates to $1x10^6$ spores/ml. Before air
187 gun infection, all isolates were mixed at equal volume and concentration.
188
189 **Preparation of *Fusarium* inoculum**
190 *F. avenaceum*, *F. culmorum* and *F. graminearum* were collected from Swedish fields in summer
191 of 2021 and characterized morphologically for species determination, and genotyped by Kaur
192 & Vilvert *et al*. (2024) using universal ITS primers ITS1 (5'-TCCGTAGGTGAACCTGCGG-
193 3') and ITS4 (5'-TCCTCCGCTTATTGATATGC-3'), and species specific primers for *F.*
194 *graminearum* marker GOFW (5'-ACCTCTGTTGTTCTTCCAGACGG-3') GORV (5'-
195 CTGGTCAGTATTAACCGTGTGTG-3'), and *F. culmorum* with marker Fc03 (5'-
196 TTCTTGCTAGGGTTGAGGATG-3') Fc02 (5'-GACCTTGACTTTGAGCTTCTTG-3')
197 (Astrid Bauer & Seigner, 2015; De Biazio *et al*., 2008). For co-infections with the three
198 *Fusarium* species, isolates were grown for two weeks at 25 °C on oatmeal agar (OMA: 3 g/L
199 organic oatmeal flower and 16 g/L agar) and sporulation was induced by exposure to natural
200 light for 3 days. For co-infections with *Z. tritici*, all *Fusarium* species were incubated in muesli
201 agar (MA: 25 g/L organic muesli: oatmeal, wheat spikes, barley and rye flakes, sunflower
202 seeds, and sunflower lecithin; 2 g/L malt extract and 12 g/L agar), and incubated at 25 °C for
203 30 days. After the incubation period, spores were collected by scratching from the plate and
204 suspended in TWEEN 0.01%. The final spore concentration was adjusted to 250 spores/µL and
205 aliquoted into vials at -20 °C until infection day.
206
207 **Coinfection assays**
208 For coinfections with different *Fusarium* species, 6 cm long leaf segments were cut from 15-
209 days-old wheat seedlings. Leaf segments were punctured and inoculated with 15 µL of a spore
210 solution at the desired concentration. For co-infections with different *Fusarium* species, an
211 equal volume and concentration of spores (10 spores/µL) were mixed into a 15 µL drop and
212 inoculated as described above. As a control, a group of leaf segments were inoculated with
213 TWEEN 0.01%. Leaf segments were placed in Benzimidazole Agar Medium (BAM: 5% water
214 agar supplemented with 0.03 mg/L benzimidazole). Custom frames made of polylactic acid
215 (PLA) were designed and 3D printed on a Flashforge Guider 2s machine (Flashforge). These
216 were used to keep the leaf surface in contact with BAM medium, preventing desiccation and

curling which happens when incubation time extends over 4-5 days. Pictures were taken at 8 dpi using a DSLR camera. Phenotyping of the commercial cultivars, lab standards, and breeding lines was performed using shorter 4 cm length leaf segments, with a spore concentration of 250 spores/µL and an incubation time of 5 days without PLA frames.

For *F. graminearum – Z. tritici* coinfections, 9-days-old wheat seedlings were placed in closed chamber made of two stacked clear PLA containers. The *Z. tritici* inoculum consisted of a mix at an equal ratio of the seven isolates described above, sprayed with a spray gun over the seedlings using 0.33 ml per seedling. As a control, a group of plants were inoculated with TWEEN 0.01%. After inoculation, the climate in the infection chamber was maintained at high humidity (over 70% of RH) and in darkness for 24 hours. Then plants were placed back in a day-night cycle as described above, and kept at high RH by spraying distilled water, using a low-pressure spray gun. Then, 6 cm length leaf segments were cut from *Z. tritici*-infected and mock-inoculated plants at 3 days post infection (dpi). Secondary infections with *F. graminearum* were performed as described above, using a 15 µL drop with a *F. graminearum* spore concentration of 250 sp/µl. Leaf segments were kept on BAM plates and maintained in darkness with high RH for 24 hours. Then, plates were moved back to a day/night cycle at high RH, incubated for 4 days (MG5323) or 5 days (Fielder), then photographed.

Machine learning-aided image analysis

Each leaf segment from the original picture was extracted individually using ImageJ. To quantify disease severity, Jupyter Notebooks were used to run code from the PlantCV and OpenCV packages (Gehan *et al*., 2017). Images showing the juxtaposition of different masks were obtained using the Jupyter Notebooks terminal interface. Bash commands were used to simultaneously analyze multiple samples from one directory with the PlantCV based script, which creates a JSON file as output for further analysis. The implementation of PlantCV allows binary image transformation from original RGB pictures, mask creation, and pixel classification in different predefined classes using a multiclass Naïve Bayes (NB) algorithm.

To define our region of interest (ROI) and reduce the error rate of the algorithm, the picture area inside the PLA frames holding the leaves was extracted. Each leaf segment was extracted as individual image using PlantCV based script (Gehan *et al*., 2017). Pixels were manually captured with ImageJ, and their RGB parameters (red, green, blue) were saved in a tab delimited file where we define each class of pixel. To avoid class imbalance, we collected the

same number of pixels for each class (necrosis, chlorosis, healthy tissue, and background). The training set consisted of over 1000 different pixels from each class. Once the RGB values of each class were defined in a training set, a Naïve Bayes (NB) algorithm (Gehan *et al*., 2017) was used to develop a probability function for each pre-defined class. After the training step, a probability function was used by the NB algorithm to classify each pixel, and the data was exported to JSON file containing the number of counted pixels in each predefined class. Data was transformed to a tabular file and uploaded to the R statistical environment for further analysis.

Statistical analysis

Data was initially tested for normality and homocedasticity, then a linear model with fixed effects was designed after performing an aligned-rank transformation with the values of necrosis or chlorosis (y) as response variable and cultivar (x_1), zymoseptoria (x_2) and its interaction (x_3) as explanatory variables with their corresponding coefficients ($\beta_1, \beta_2, \beta_3$). The constant μ represents the intercept.

$$y = \mu + \beta_1 x_1 + \beta_2 x_2 + \beta_3 x_3$$

To test statistical differences, we performed an aligned-rank-transformation-two-way-ANOVA (robust two-way-ANOVA) and a *post hoc* test with Tukey adjustment. A Principal Component Analysis (PCA) was carried out with the average value of each cultivar and *Fusarium* species combination (each combination has at least 5 biological replicates). Coordinates of each sample in the PCA were extracted to calculate the distance matrix which was used as input for cluster analysis using a Hierarchical Agglomerative Nesting (AGNES) algorithm. All statistical analyses were performed with R (version 4.2.2) in the Rstudio environment (R Core Team, 2022) and the packages: readxl, dplyr, tidyr, stringr, reshape2, ggplot2, multcompView, forcats, ARTool, rcompanion, factoextra, and cluster (Graves *et al*., 2023; Kassambara & Mundt, 2020; Kay *et al*., 2021; Maechler *et al*., 2022; Mangiafico, 2023; Wickham, *et al*., 2023; Wickham, *et al*., 2023; Wickham, 2007, 2016, 2022, 2023; Wickham & Bryan, 2023).

Results

Phenotypic analysis of single *vs.* mixed *Fusarium* species infection of wheat leaves

We selected the bread wheat cultivar Fielder for this assay based on the consistent and clear phenotypes we obtained in our preliminary tests and our previous work (Kaur and Vilvert, *et al*. 2024). We adapted a leaf segment infection strategy based on previous work demonstrating

284 high correlation between the phenotypes observed in leaf segment assays and quantitative
285 disease resistance to FHB in the field (Kumar et al., 2011; Perochon & Doohan, 2016). Leaf
286 segments were inoculated with *F. avenaceum*, *F. culmorum*, *F. graminearum* and their
287 combinations by drop inoculation (see Methods). At 8 dpi, variability in disease severity among
288 the different pathogens and their combinations was assessed by eye (**Figure 2**). Here, we
289 reasoned that if interactions between *Fusarium* species are a major component of how these
290 species act in a complex, then such assay should lead to clear differential phenotypes i.e.
291 observable by a trained person. Indeed, *F. graminearum* showed the most severe symptoms,
292 triggering necrosis in large areas of the leaf segment. By contrast, the combination of *F.*
293 *culmorum* and *F. graminearum* caused much weaker symptoms as compared to single
294 infections with *F. graminearum*. These results suggest that *F. graminearum* is the most
295 aggressive of the three *Fusarium* species tested, and that there are interactions among *F.*
296 *avenaceum*, *F. culmorum* and *F. graminearum* that could change the plant response and or
297 directly affect complex assembly. We conclude that the detached leaf assay is sensitive to
298 *Fusarium* species composition and can reveal quantitative difference in disease severity
299 resulting from pure *vs*. mixed species inocula.
300
301 **Precision phenotyping using Image-based quantification of disease severity**
302 In another series of experiments, we aimed at developing an image-based precision
303 phenotyping strategy to distinguish and quantify two important components of the observed
304 symptoms, namely: necrosis and chlorosis. We reasoned that these two types of tissue
305 alterations denote different physiological processes taking place during the progression of
306 disease, and their prevalence may vary between genotypes thus pinpointing to distinctly
307 different host factors involved in the response to *Fusarium* sp. We analyzed the pictures using
308 a NB algorithm trained with a set of RGB values from different pixels classified as 'necrosis',
309 'chlorosis', 'healthy tissue' and 'background' (see Methods). We used a test set of 64 leaf
310 segment pictures to test this approach. We were able to clearly separate each type of tissue, and
311 create so called 'masks' (see Methods) allowing the visualization and the quantification of the
312 infected area undergoing necrosis *vs*. chlorosis (**Figure 3**). The results of the quantification of
313 each leaf segment grouped by treatment are illustrated in **Figure 4**. They also could validate
314 that the script correctly identified the infection with *F. graminearum* as the infection which
315 triggers the most severe response (the highest amount of necrotic tissue). The levels of necrosis
316 observed in the control group are close to 0, indicating a high performance of the classifier
317 algorithm. We could also corroborate and quantify the cases where mixed infection resulted in

less necrosis than infection with a pure culture of *F. graminearum*. Altogether, we conclude that our image-based, machine learning aided phenotyping pipelines can correctly and precisely quantify disease symptoms and reveal the smallest differences in the wheat response to single *vs*. mixed *Fusarium* inocula.

Comparison of disease severity values scored visually *vs.* using machine-learning

We then compared the disease scoring obtained from a trained person with the results obtained with machine-learning (ML) aided image analysis. Here, we aimed at identifying the added value of accurate segmentation of the phenotype into necrosis and chlorosis (i.e. expressed as a percentage), which we argued are very difficult to separate from the composite disease phenotype scored by eye (expressed as a scale from 1 to 5). We used an image library previously generated by us (Kaur and Vilvert., *et al*, 2024). It consisted of images of detached leaf infection assays with *F. avenaceum*, *F. culmorum*, *F. graminearum* and their combinations in a panel of different wheat lines. Due to the large number of putative comparisons (39 lines and 7 different treatments) and considering the complexity of the data, we decided to perform an exploratory cluster analysis with the coordinates of each sample obtained in a PCA and compare the relative position of each cultivar.

We found that the most coherent clustering was obtained with the percentage of necrosis scored by ML based on a Naïve Bayes algorithm (**Figure 5, Supplementary Tables 2, 3, 4, 5**). This approximation aggregates the samples in the breeding lines (blue), lab standards (pink) and commercial lines (green, red and yellow). Moreover, the clusters obtained with the values of necrosis percentage are similar to the groups obtained with visual scores. In both cases there are two clear groups of commercial lines close to the lab standard and the breeding lines (blue and yellow in manual scoring and orange and yellow in ML scoring), and a third commercial line group which is less similar to the lab standards (green, ML scoring), which is split in two closely related groups in the manual scoring (green and pink). In contrast, with manual scoring, the parental lines are spread between the cluster of lab standards (Latino, Zardak and MG5323, tetraploid durum wheat) and one of the clusters of commercial lines (Artico, Victo and Agadir, hexaploid wheat). However, beyond these differences, the relative position of each line in comparison with the others remains relatively similar. For example, the lab standard Fielder is close to Chinese Spring, Bob-White, Eleven, Amulett, and Rogue in both cases, with manual scoring and with necrosis calculated with Naïve Bayes algorithm. In summary, we found that the ML-based scoring allowed better defined clusters differentiating the different genotypes

352 used in this study. These results further indicate that the ML strategy surpassed the visual
353 scoring in terms of (i) tissue segmentation accuracy, (ii) sensitivity to small differences, and
354 (iii) precise quantification of different tissue types, all of which are of paramount importance
355 for clustering genotypes based on similar disease responses.
356
357 We then performed a robust ANOVA analysis (**Supplementary Table 6**), to detect statistically
358 significant differences between different groups of cultivars vs. treatments. The results of the
359 ANOVA indicate that observed differences (i.e. as in the clustering) between the groups of
360 cultivars, *Fusarium* combinations and the combination of both, are statistically significant ($p <$
361 0.01). This further demonstrates that our strategy can detect single *Fusarium* species and
362 *Fusarium* complex-specific responses in a cultivar-dependent manner, which is an important
363 validation of our strategy as a potential tool for mapping host factors underlying FHB complex
364 assembly in wheat.
365
366 **Phenotypic analysis of the effect of primary infection with *Z. tritici* on *F. graminearum***
367 In a recent study by us we could demonstrate that *Fusarium* taxa commonly implicated in FHB
368 largely co-exist with wheat leaves showing blotch symptoms typically caused by *Z. tritici* in
369 Sweden (Kaur and Vilvert, *et al*, 2024). We further isolated several isolates of *F. graminearum*
370 and *F. culmorum* from typical blotch-like necrotic lesions, and demonstrated using our leaf
371 segment assays that they can indeed cause blotch-like symptoms that can be easily confound
372 with *Z. tritici*, or *Pyrenophora-tritici repentis* (Kaur and Vilvert, *et al*, 2024). We thus aimed at
373 developing a phenotyping strategy that would allow us to explore these intriguing interactions
374 between *Z. tritici* and *Fusarium* spp.
375
376 We used cultivar Fielder, a universal susceptible control for *Z. tritici* which has also been the
377 basis for our leaf segment infection assays with *F. graminearum*. We used a mix at equal ratio
378 of seven *Z. tritici* isolates representing genotypes with a broad and non-overlapping spectrum
379 of virulence originating from an extensively characterized population developed at ETH Zurich
380 (Zhan *et al*., 2003, 2005). Considering the high genetic diversity of *Z. tritici* populations
381 commonly present in a single field, we reasoned that our assays would gain in biological
382 relevance may we integrate a higher-level of inoculum complexity. We also used *F.*
383 *graminearum*, as it was the *Fusarium* specie which resulted in the most severe symptoms in
384 our assay.
385

386 First, we checked the sensitivity of the image analysis strategy to detect dose-dependent effects
387 where *F. graminearum* inoculations were done at 10, 100 and 250 spores/µl on material that
388 was initially infected with *Z. tritici* (see Methods, **Figure 6A**). The NB algorithm recognized
389 higher levels of necrosis and chlorosis in leaf segments infected at a concentration of 10
390 spores/µl in comparison with the negative controls, although the differences are not consistent
391 enough to be statistically significant (**Figure 6B**). Leaf segments inoculated with a
392 concentration of 100 and 250 spores/µl showed similar levels of necrosis and chlorosis,
393 although higher concentrations tend to give more severe disease symptoms (**Figure 6B, 6C**).
394 Most importantly, we also detected a reduction of the necrosis and chlorosis caused by *F.*
395 *graminearum* on the leaf segments pre-infected with *Z. tritici* (**Figure 6B**). It is noteworthy
396 that, considering the timing of the co-infections, the observed interactions are taking place
397 during the biotrophic phase of the hemibiotrophic lifestyle of *Z. tritici*. Therefore, these results
398 suggest there is possible antagonism from *Z. tritici*, during its biotrophic stage, to suppress the
399 necrotic lifestyle of *F. graminearum*, which can be detected by our strategy.
400
401 To further explore the capacity of our pipeline to reveal such phenotypes, we expanded our
402 analysis to one tetraploid wheat accession (MG5323) which has been consistently more
403 susceptible to *F. graminearum* leaf infections than Fielder in our assays. We wanted to assess
404 if an inhibitory effect from *Z. tritici* would still be visible provided with higher virulence from
405 *F. graminearum* on the host. Here, comparisons between MG5323 and Fielder come handy as
406 both genotypes are susceptible to *Z. tritici*, thus the outcome of interactions should be mainly
407 influenced by the virulence level of *F. graminearum*.
408
409 The results from the image analysis show that our pipeline can still detect an inhibitory effect
410 of *Z. tritici* on *F. graminaerum* (**Figure 7A**), however, this effect is weaker in MG5323 where
411 *F. graminearum* is more virulent (**Figure 7B**). We also observed that such an effect seems to
412 preferentially act on necrosis rather than chlorosis in Fielder, where inhibition allows more
413 refined phenotypic readout. On the contrary, the effect on chlorosis was more prominent in
414 MG5323 where we were able to detect a statistically significant reduction in presence of *Z.*
415 *tritici*. Together, these results suggest that *Z. tritici* can modify the host response to *F.*
416 *graminearum* which seems to be conserved across different wheat species. We propose that
417 such mechanisms are likely to alter the endophytic lifestyle of the *Fusarium* species thus
418 playing a possible role in shaping *Fusarium* populations in the field.
419

420 **Discussion**

421 In this study we presented an original experimental set up allowing the study of disease
422 interactions in wheat with a focus on FHB. Detached leaf assays are highly suitable for large
423 scale screens due to the relatively short time from seed to inoculation, and the low requirements
424 of space. In fact, the full procedure can be performed in 17 days thus facilitating the screening
425 of large populations. Several procedures have been developed to phenotype resistance to FHB
426 ranging from spikelet infection in the lab and in the field (Chhabra *et al*., 2024; Giancaspro *et*
427 *al*., 2016), *in vitro* detached head inoculation (Huang *et al*., 2020), seedling assays (Soresi *et*
428 *al*., 2015), coleoptile infection assays (Wu *et al*., 2005), and detached leaf assay (Perochon &
429 Doohan, 2016). Even though detached leaf assays are commonly used, precision phenomics
430 strategies to quantify the resulting phenotypes have not been exploited, with a few attempts
431 restricted to the measurement of lesion diameter (Perochon & Doohan, 2016; Roesler *et al*.,
432 2022). A major feature of our strategy is the possibility to simultaneously decompose the
433 symptoms into two types of alterations (necrosis and chlorosis) and precisely (i.e. to the pixel)
434 measure their relative areas. Furthermore, we demonstrate that there are measurable differences
435 in the ability of FHB associated taxa to cause either of these symptoms on different genotypes
436 (alone or in combination). Thus, in this work, we took full advantage of such reductionist
437 approaches to explore the complexity of multi-pathogen species interactions within the FHB
438 complex, and between FHB and other wheat pathogens.

439

440 The first interesting finding of this work was the inherent variation in the capacity of different
441 FHB associated *Fusarium* species to induce chlorosis or necrosis. While the mechanisms
442 underlying the expression of these tissue alterations are conserved among plants, their
443 physiological basis is very different. Chlorosis is typically a nutrient deficiency phenotype
444 commonly induced when micronutrients such as iron (Fe) and zinc (Zn) are depleted from the
445 cells (Nogiya *et al*., 2016). Chlorosis is not to be confused with 'senescence' which is a highly
446 regulated developmental process in plants which may also result from nutrient deficiency (i.e.
447 starvation) but is largely controlled by genetic programming (Noodén *et al*., 1997). Necrosis is
448 a typical marker for biotic stress, triggered by the plant immune system in response to
449 pathogens (Minina *et al*., 2005). In this context, our results indicated that FHB associated
450 species have different abilities to differentially alter two highly conserved tissue damage-
451 associated mechanisms reminiscent of blight symptoms. This could indicate a form of
452 functional specialization among species of the FHB complex.

453

454 Furthermore, we showed that the ability to cause these symptoms and their relative prevalence
455 is genotype-specific, and species combination-dependent. Such genotype-specific variation in
456 the hemibiotrophic lifestyle was also observed in other pathogenic *Fusarium* species such as
457 *F. temperatum*, and *F. oxysporum* (Hill *et al*., 2022; Robles-Barrios *et al*., 2022; Srivastava *et*
458 *al*., 2024). We therefore speculate that such variation may reflect dynamic changes in the
459 hemibiotrophic lifestyle of *Fusarium* sp. Here, a classical progression would correspond to an
460 early endophytic colonization without visible symptoms, followed by the induction of chlorosis
461 as nutrients are gradually depleted by the fungus, then a shift to a necrotrophic lifestyle where
462 the pathogen switches to feeding on dead tissues. Thus, what our assay could be revealing a
463 possibly new types of resistance to FHB based on the suppression of deleterious tissue
464 alterations by chlorosis and necrosis.
465
466 Another interesting finding from this study was the observation that co-existence of different
467 *Fusarium* species can have a measurable negative impact on the performance of the complex
468 to cause lesions on the leaves. In fact, we found a statistically significant difference between
469 single *F. graminearum* infections and inoculations with *F. culmorum* and *F. graminearum*. This
470 is counter intuitive considering that disease complexes such as FHB are largely considered as
471 based on a form of synergism between microbial pathogens (Lamichhane & Venturi, 2015).
472 This is for instance represented in our assays by the *F. avenaceum* and *F. graminearum*
473 combination, which tends to have a higher disease severity than *F. avenaceum* single infection.
474 Similarly, evidence shows that co-infection with *F. aglaonematis sp. nov.* and *F. elaeidis*
475 triggers more severe disease symptoms in *Aglaonema modestum* as compared with single
476 infections (Zhang *et al*., 2022). This further highlight the difficulty to predict multispecies-
477 complex dynamics, which are proposed to result from evolutionary competition and pathogen
478 niche specialization (Abdullah *et al*., 2017).
479
480 Altogether these observations may indicate that the ability of taxa from the FHB complex to
481 cooperate *vs*. compete may have a fitness cost which could be partially determined by the host.
482 Such cost could for instance be associated with tradeoffs between the maintenance of virulence
483 factors important to infect the host vs. antimicrobial factors important for competition with
484 other taxa in the complex. Numerous studies showing that filamentous plant pathogens
485 significantly impact the host microbiome, and recent discoveries suggesting that pathogen
486 genomes encode large arrays of so-called effectors which are primarily targeted to outcompete
487 other microbes (Flores-Nunez & Stukenbrock, 2024; Snelders et al., 2022). While at the same

time, it was also shown that the maintenance of such large repertoire of virulence factors can also have an impact on pathogen fitness (Montarry et al., 2010). These observations are highly relevant for the cases where we saw possible signs of competition over plant immunity and plant resources in two cases where *F. graminearum* was combined with another *Fusarium* species or *Z. tritici*. This is also consistent with previous studies demonstrating that both *F. greaminearum* and *Z. tritici* have the capacity to manipulate the plant microbiome during infection, including the identification of specific effector proteins with antifungal activity in from *Z. tritici* (Kettles et al., 2018; Rojas et al., 2020). In fact, competition between *Fusarium* species as a strategy for biological control has been discussed and tested with some success (Aimé *et al*., 2013; Alabouvette *et al*., 2009).

We therefore conclude that the ability to reveal differences in the plant immune response to single vs. species infection is an important step forward in understanding the factors controlling FHB complex assembly, which further demonstrates the future potential of our experimental pipeline to be used a genetic tool for resistance screening.

Data availability

All data is available within the manuscript or in the supplementary material. Additional information will be made available upon request to the corresponding author.

Funding

This was supported by funding from the Swedish Research Council for Sustainable Development FORMAS (grant number 2020-01007) and the Carl Trygger Foundation (grant number 21:1171).

Conflict of interest statement:

The authors have no conflicts of interest to declare.

Aknowledgment

We would like to acknowledge Fredric Hedlund and Ayano Tanaka for technical assistance with the growth facilities at SLU Biocentrum. We would also like to acknowledge the support of the Plant Protection Extensions 'Växtskyddscentralerna' of the Swedish Board of Agriculture 'Jordbruksverket' (https://jordbruksverket.se/) with field sampling across Sweden. We also thank Katarina Ihrmark and Maria Jonsson for their technical assistance.

522 **References**

523 Abdullah, A. S., Moffat, C. S., Lopez-Ruiz, F. J., Gibberd, M. R., Hamblin, J., & Zerihun, A.
524 (2017). Host–multi-pathogen warfare: Pathogen interactions in co-infected plants.
525 *Frontiers in Plant Science*, *8*(October), 1–12. https://doi.org/10.3389/fpls.2017.01806
526 Aimé, S., Alabouvette, C., Steinberg, C., & Olivain, C. (2013). The endophytic strain
527 Fusarium oxysporum Fo47: A good candidate for priming the defense responses in
528 tomato roots. *Molecular Plant-Microbe Interactions*, *26*(8), 918–926.
529 https://doi.org/10.1094/MPMI-12-12-0290-R
530 Alabouvette, C., Olivain, C., Migheli, Q., & Steinberg, C. (2009). Microbiological control of
531 soil-borne phytopathogenic fungi with special emphasis on wilt-inducing Fusarium
532 oxysporum. *New Phytologist*, *184*(3), 529–544. https://doi.org/10.1111/j.1469-
533 8137.2009.03014.x
534 Alisaac, E., & Mahlein, A. K. (2023). Fusarium Head Blight on Wheat: Biology, Modern
535 Detection and Diagnosis and Integrated Disease Management. *Toxins*, *15*(3).
536 https://doi.org/10.3390/toxins15030192
537 Astrid Bauer, R. S., & Seigner, L. (2015). Detection, Identification and Quantification of
538 Fusarium graminearum and Fusarium culmorum in Wheat Kernels by PCR Techniques.
539 *Journal of Plant Pathology & Microbiology*, *06*(07). https://doi.org/10.4172/2157-
540 7471.1000287
541 Audenaert, K., van Broeck, R., van Bekaert, B., de Witte, F., Heremans, B., Messens, K.,
542 Höfte, M., & Haesaert, G. (2009). Fusarium head blight (FHB) in Flanders: Population
543 diversity, inter-species associations and DON contamination in commercial winter
544 wheat varieties. *European Journal of Plant Pathology*, *125*(3), 445–458.
545 https://doi.org/10.1007/s10658-009-9494-3
546 Browne, R. A., & Cooke, B. M. (2005). Resistance of wheat to Fusarium spp. in an in vitro
547 seed germination assay and preliminary investigations into the relationship with
548 Fusarium head blight resistance. *Euphytica*, *141*(1–2), 23–32.
549 https://doi.org/10.1007/s10681-005-4820-0
550 Burgess, L. W., Klein, T. A., Bryden, W. L., & Tobin, N. F. (1987). Head blight of wheat
551 caused by Fusarium graminearum Group 1 in New South Wales in 1983. *Australasian*
552 *Plant Pathology*, *16*(72).
553 Chhabra, B., Thrasu, S., Wallace, S., Schoen, A., Shahoveisi, F., Dong, Y., Tiwari, V., &
554 Rawat, N. (2024). Evaluation of speed breeding conditions for accelerating Fusarium
555 head blight and deoxynivalenol screening in wheat. *Crop Science*, *64*(3), 1586–1594.

https://doi.org/10.1002/csc2.21226

Collinge, D. B., Jensen, B., & Jørgensen, H. J. (2022). Fungal endophytes in plants and their relationship to plant disease. *Current Opinion in Microbiology*, *69*, 102177. https://doi.org/10.1016/j.mib.2022.102177

De Biazio, G. R., Leite, G. G. S., Tessmann, D. J., & Barbosa-Tessmann, I. P. (2008). A new PCR approach for the identification of Fusarium graminearum. *Brazilian Journal of Microbiology*, *39*(3), 554–560. https://doi.org/10.1590/s1517-83822008000300028

Diamond, H., & Cooke, B. M. (1999). Towards the development of a novel in vitro strategy for early screening of Fusarium Ear Blight resistance in adult winter wheat plants. *Pest Management Focus*, *5*(1), 2.

Doohan, F. M., Brennan, J., & Cooke, B. M. (2003). Influence of climatic factors on Fusarium species pathogenic to cereals. *European Journal of Plant Pathology*, *109*(7), 755–768. https://doi.org/10.1023/A:1026090626994

Flores-Nunez, V. M., & Stukenbrock, E. H. (2024). The impact of filamentous plant pathogens on the host microbiota. *BMC Biology*, *22*(1), 1–11. https://doi.org/10.1186/s12915-024-01965-3

Gehan, M. A., Fahlgren, N., Abbasi, A., Berry, J. C., Callen, S. T., Chavez, L., Doust, A. N., Feldman, M. J., Gilbert, K. B., Hodge, J. G., Hoyer, J. S., Lin, A., Liu, S., Lizárraga, C., Lorence, A., Miller, M., Platon, E., Tessman, M., & Sax, T. (2017). PlantCV v2: Image analysis software for high-throughput plant phenotyping. *PeerJ*, *2017*(12), 1–23. https://doi.org/10.7717/peerj.4088

Gerling, M., Petry, L., Barkusky, D., Büttner, C., & Müller, M. E. H. (2023). Infected grasses as inoculum for Fusarium infestation and mycotoxin accumulation in wheat with and without irrigation. *Mycotoxin Research*, *39*(1), 19–31. https://doi.org/10.1007/s12550-022-00470-2

Giancaspro, A., Giove, S. L., Zito, D., Blanco, A., & Gadaleta, A. (2016). Mapping QTLs for Fusarium head blight resistance in an interspecific wheat population. *Frontiers in Plant Science*, *7*(September2016), 1–13. https://doi.org/10.3389/fpls.2016.01381

Graves, S., Piepho, H.-P., & with help from Sundar Dorai-Raj, L. S. (2023). *multcompView: Visualizations of Paired Comparisons*. https://cran.r-project.org/package=multcompView

Hill, R., Buggs, R. J. A., Vu, D. T., & Gaya, E. (2022). Lifestyle Transitions in Fusarioid Fungi are Frequent and Lack Clear Genomic Signatures. *Molecular Biology and Evolution*, *39*(4), 1–19. https://doi.org/10.1093/molbev/msac085

590 Huang, C., Gangola, M. P., Randy Kutcher, H., Hucl, P., Ganeshan, S., & Chibbar, R. N.
591 (2020). In vitro wheat immature spike culture screening identified fusarium head blight
592 resistance in wheat spike cultured derived variants and in the progeny of their crosses
593 with an elite cultivar. *Plant Pathology Journal*, *36*(6), 558–569.
594 https://doi.org/10.5423/PPJ.OA.07.2020.0127
595 Karlsson, I., Persson, P., & Friberg, H. (2021). Fusarium Head Blight From a Microbiome
596 Perspective. *Frontiers in Microbiology*, *12*(March), 1–17.
597 https://doi.org/10.3389/fmicb.2021.628373
598 Kassambara, A., & Mundt, F. (2020). *factoextra: Extract and Visualize the Results of*
599 *Multivariate Data Analyses*. https://cran.r-project.org/package=factoextra
600 Kaur, H., Vilvert, E., Corrales Gutiérrez, M. Á., Zhan, J., Douchkov, D., Desiderio, F., Vélez,
601 H., & Bourras, S. (2024). Diagnostic of head blight and leaf blotch diseases of wheat in
602 Sweden using a mycobiome isolation approach. *BioRxiv*.
603 Kaur, H., Vilvert, E., Corrales Gutiérrez, M. Á., Zhan, J., Douchkov, D., Desiderio, F., Vélëz,
604 H., & Salim, B. (2024). Survey of the wheat mycobiome associated with leaf blotch and
605 head blight diseases in Sweden. *BiorXiv*.
606 Kaur, H., Vilvert, E., Gutiérrez, M. Á. C., Zhan, J., Douchkov, D., Desiderio, F., Vélëz, H., &
607 Bourras, S. (2024). Survey of the wheat mycobiome associated with leaf blotch and head
608 blight diseases in Sweden. *BioRxiv*, 2024.01.09.574850.
609 https://www.biorxiv.org/content/10.1101/2024.01.09.574850v1%0Ahttps://www.biorxiv
610 .org/content/10.1101/2024.01.09.574850v1.abstract
611 Kay, M., Elkin, L. A., Higgins, J. J., & Wobbrock, J. O. (2021). *{ARTool}: Aligned Rank*
612 *Transform for Nonparametric Factorial ANOVAs*.
613 https://doi.org/10.5281/zenodo.594511
614 Kazan, K., & Gardiner, D. M. (2018). Fusarium crown rot caused by Fusarium
615 pseudograminearum in cereal crops: recent progress and future prospects. *Molecular*
616 *Plant Pathology*, *19*(7), 1547–1562. https://doi.org/10.1111/mpp.12639
617 Kettles, G. J., Bayon, C., Sparks, C. A., Canning, G., Kanyuka, K., & Rudd, J. J. (2018).
618 Characterization of an antimicrobial and phytotoxic ribonuclease secreted by the fungal
619 wheat pathogen Zymoseptoria tritici. *New Phytologist*, *217*(1), 320–331.
620 https://doi.org/10.1111/nph.14786
621 Khan, M. K., Pandey, A., Athar, T., Choudhary, S., Deval, R., Gezgin, S., Hamurcu, M.,
622 Topal, A., Atmaca, E., Santos, P. A., Omay, M. R., Suslu, H., Gulcan, K., Inanc, M.,
623 Akkaya, M. S., Kahraman, A., & Thomas, G. (2020). Fusarium head blight in wheat:

contemporary status and molecular approaches. *3 Biotech*, *10*(4), 1–17. https://doi.org/10.1007/s13205-020-2158-x

Kumar, K., Xi, K., Turkington, T. K., Tekauz, A., Helm, J. H., & Tewari, J. P. (2011). Evaluation of a detached leaf assay to measure fusarium head blight resistance components in barley. *Canadian Journal of Plant Pathology*, *33*(3), 364–374. https://doi.org/10.1080/07060661.2011.590820

Lamichhane, J. R., & Venturi, V. (2015). Synergisms between microbial pathogens in plant disease complexes: A growing trend. *Frontiers in Plant Science*, *6*(MAY), 1–12. https://doi.org/10.3389/fpls.2015.00385

Lidia, B., Sylwia, S., & Katarzyna, M. (2021). Fungi inhabiting the wheat endosphere. *Pathogens*, *10*(10). https://doi.org/10.3390/pathogens10101288

Lukanowski, A., Lenc, L., & Sadowski, C. (2008). First report on the occurrence of Fusarium langsethiae isolated from wheat kernels in Poland. *Plant Disease*, *92*(3), 488. https://doi.org/10.1094/PDIS-92-3-0488A

Ma, L. J., Kistler, H. C., & Rep, M. (2013). Evolution of Plant Pathogenicity in Fusarium Species. *Evolution of Virulence in Eukaryotic Microbes*, 485–500. https://doi.org/10.1002/9781118308165.ch26

Maechler, M., Rousseeuw, P., Struyf, A., Hubert, M., & Hornik, K. (2022). *cluster: Cluster Analysis Basics and Extensions*. https://cran.r-project.org/package=cluster

Maina Wagacha, J., Njeru, N. K., Otieno Okumu, O., Muthomi, J. W., Mutegi, C. K., Wagacha, J. M., & Okumu, O. O. (2016). Occurrence of Fusarium Head Blight of Wheat and Associated Mycotoxins in Narok and Nakuru Counties, Kenya. *World Journal of Agricultural Research*, *4*(4), 119–127. https://doi.org/10.12691/wjar-4-4-4

Mangiafico, S. S. (2023). *{rcompanion}: Functions to Support Extension Education Program Evaluation*. https://cran.r-project.org/package=rcompanion/

Mesterhazy, A. (1987). Selection of Head Blight Resistant Wheats Through Improved Seedling Resistance. *Plant Breeding*, *98*(1), 25–36. https://doi.org/10.1111/j.1439-0523.1987.tb01086.x

Mesterhazy, A. (2020). Updating the Breeding Philosophy of Wheat to. *Plants*, *9*(1702), 33.

Minina, E. A., Filonova, L. H., Sachez-Vera, V., Suarez, M. F., Gepffrey, D., & Bozhkov, P. V. (2005). Detection and Measurement of Necrosis in Plants. In *Methods of Biochemical Analysis* (Vol. 47).

Montarry, J., Hamelin, F. M., Glais, I., Corbi, R., & Andrivon, D. (2010). Fitness costs associated with unnecessary virulence factors and life history traits: Evolutionary

insights from the potato late blight pathogen Phytophthora infestans. *BMC Evolutionary Biology*, *10*(1). https://doi.org/10.1186/1471-2148-10-283

Niks, R., & Skinnes, H. (1998). Airbone pathogens on cereals. In B. Cooke (Ed.), *Airbone pathogens on cereals*. Office for Official Publications of the European Communities.

Nogiya, M., Pandey, R. N., & Singh, B. (2016). Physiological basis of iron chlorosis tolerance in rice (Oryza sativa) in relation to the root exudation capacity. *Journal of Plant Nutrition*, *39*(11), 1536–1546. https://doi.org/10.1080/01904167.2016.1161786

Noodén, L. D., Guiamét, J. J., & John, I. (1997). Senescence mechanisms. *Physiologia Plantarum*, *101*(4), 746–753. https://doi.org/10.1034/j.1399-3054.1997.1010410.x

Obanor, F., & Chakraborty, S. (2014). Aetiology and toxigenicity of fusarium graminearum and F. pseudograminearum causing crown rot and head blight in Australia under natural and artificial infection. *Plant Pathology*, *63*(6), 1218–1229. https://doi.org/10.1111/ppa.12200

Obanor, F., Neate, S., Simpfendorfer, S., Sabburg, R., Wilson, P., & Chakraborty, S. (2013). Fusarium graminearum and Fusarium pseudograminearum caused the 2010 head blight epidemics in Australia. *Plant Pathology*, *62*(1), 79–91. https://doi.org/10.1111/j.1365-3059.2012.02615.x

Parry, D. W., Jenkinson, P., & McLeod, L. (1995). Fusarium ear blight (scab) in small grain cereals—a review. *Plant Pathology*, *44*(2), 207–238. https://doi.org/10.1111/j.1365-3059.1995.tb02773.x

Perochon, A., & Doohan, F. (2016). Assessment of Wheat Resistance to Fusarium graminearum by Automated Image Analysis of Detached Leaves Assay. *Bio-Protocol*, *6*(24). https://doi.org/10.21769/bioprotoc.2065

R Core Team. (2022). *R: A Language and Environment for Statistical Computing*. https://www.r-project.org/

Redkar, A., Sabale, M., Zuccaro, A., & Di Pietro, A. (2022). Determinants of endophytic and pathogenic lifestyle in root colonizing fungi. *Current Opinion in Plant Biology*, *67*, 102226. https://doi.org/10.1016/j.pbi.2022.102226

Robles-Barrios, F., Ramírez-Granillo, A., Medina-Canales, M. G., Gómez-Lim, M., Loske, A. M., Rodríguez-Tovar, A. V., & Pérez, N. O. (2022). Fusarium temperatum shows a hemibiotrophic infection process and differential pathogenicity over different maize breeds from Mexico. *Journal of Phytopathology*, *170*(1), 21–33. https://doi.org/10.1111/jph.13052

Roesler, E. A., Balbinott, N., Schroeder, R. G., Yamazaki-Lau, E., Lima, M. I. P. M.,

Brammer, S. P., Aragão, F. J. L., Fernandes, J. M. C., & Deuner, C. C. (2022). An efficient protocol for inoculation of Fusarium graminearum in detached leaves of Arabidopsis. *Tropical Plant Pathology*, *47*(3), 353–361. https://doi.org/10.1007/s40858-022-00497-x

Rojas, E. C., Sapkota, R., Jensen, B., Jørgensen, H. J. L., Henriksson, T., Jørgensen, L. N., Nicolaisen, M., & Collinge, D. B. (2020). Fusarium Head Blight Modifies Fungal Endophytic Communities During Infection of Wheat Spikes. *Microbial Ecology*, *79*(2), 397–408. https://doi.org/10.1007/s00248-019-01426-3

Rovenich, H., Boshoven, J. C., & Thomma, B. P. H. J. (2014). Filamentous pathogen effector functions: Of pathogens, hosts and microbiomes. *Current Opinion in Plant Biology*, *20*, 96–103. https://doi.org/10.1016/j.pbi.2014.05.001

Saijo, Y., Loo, E. P. iian, & Yasuda, S. (2018). Pattern recognition receptors and signaling in plant–microbe interactions. *Plant Journal*, *93*(4), 592–613. https://doi.org/10.1111/tpj.13808

Seybold, H., Demetrowitsch, T. J., Hassani, M. A., Szymczak, S., Reim, E., Haueisen, J., Lübbers, L., Rühlemann, M., Franke, A., Schwarz, K., & Stukenbrock, E. H. (2020). A fungal pathogen induces systemic susceptibility and systemic shifts in wheat metabolome and microbiome composition. *Nature Communications*, *11*(1), 1–12. https://doi.org/10.1038/s41467-020-15633-x

Snelders, N. C., Rovenich, H., & Thomma, B. P. H. J. (2022). Microbiota manipulation through the secretion of effector proteins is fundamental to the wealth of lifestyles in the fungal kingdom. *FEMS Microbiology Reviews*, *46*(5), 1–16. https://doi.org/10.1093/femsre/fuac022

Soresi, D., Garayalde, A., Zappacosta, D., & Miranda, R. (2015). An in vitro assay for pre-screening resistance to fusarium head blight in durum wheat. *Phytopathologia Mediterranea*, *54*(2), 253–264. https://doi.org/10.14601/Phytopathol

Srivastava, V., Patra, K., Pai, H., Aguilar-Pontes, M. V., Berasategui, A., Kamble, A., Di Pietro, A., & Redkar, A. (2024). Molecular Dialogue During Host Manipulation by the Vascular Wilt Fungus Fusarium oxysporum. *Annual Review of Phytopathology*, *62*(1), 97–126. https://doi.org/10.1146/annurev-phyto-021722-034823

Steiner, B., Buerstmayr, M., Michel, S., Schweiger, W., Lemmens, M., & Buerstmayr, H. (2017). Breeding strategies and advances in line selection for Fusarium head blight resistance in wheat. *Tropical Plant Pathology*, *42*(3), 165–174. https://doi.org/10.1007/s40858-017-0127-7

Stotz, H. U., Mitrousia, G. K., de Wit, P. J. G. M., & Fitt, B. D. L. (2014). Effector-triggered defence against apoplastic fungal pathogens. *Trends in Plant Science*, *19*(8), 491–500. https://doi.org/10.1016/j.tplants.2014.04.009

Sweany, R. R., Breunig, M., Opoku, J., Clay, K., Spatafora, J. W., Drott, M. T., Baldwin, T. T., & Fountain, J. C. (2022). Why Do Plant-Pathogenic Fungi Produce Mycotoxins? Potential Roles for Mycotoxins in the Plant Ecosystem. *Phytopathology*, *112*(10), 2044–2051. https://doi.org/10.1094/PHYTO-02-22-0053-SYM

Valverde-Bogantes, E., Bianchini, A., Herr, J. R., Rose, D. J., Wegulo, S. N., & Hallen-Adams, H. E. (2020). Recent population changes of Fusarium head blight pathogens: drivers and implications. *Canadian Journal of Plant Pathology*, *42*(3), 315–329. https://doi.org/10.1080/07060661.2019.1680442

Venske, E., dos Santos, R. S., Farias, D. da R., Rother, V., da Maia, L. C., Pegoraro, C., & Costa de Oliveira, A. (2019). Meta-analysis of the QTLome of fusarium head blight resistance in bread wheat: Refining the current puzzle. *Frontiers in Plant Science*, *10*(June), 1–19. https://doi.org/10.3389/fpls.2019.00727

Waalwijk, C., Kastelein, P., De Vries, I., Kerényi, Z., Van Der Lee, T., Hesselink, T., Köhl, J., & Kema, G. (2003). Major changes in Fusarium spp. in wheat in the Netherlands. *European Journal of Plant Pathology*, *109*(7), 743–754. https://doi.org/10.1023/A:1026086510156

Wickham, H. (2007). Reshaping Data with the {reshape} Package. *Journal of Statistical Software*, *21*(12), 1–20. http://www.jstatsoft.org/v21/i12/

Wickham, H. (2016). *ggplot2: Elegant Graphics for Data Analysis*. Springer-Verlag New York. https://ggplot2.tidyverse.org

Wickham, H. (2022). *stringr: Simple, Consistent Wrappers for Common String Operations*. https://cran.r-project.org/package=stringr

Wickham, H. (2023). *forcats: Tools for Working with Categorical Variables (Factors)*. https://cran.r-project.org/package=forcats

Wickham, H., & Bryan, J. (2023). *readxl: Read Excel Files*. https://cran.r-project.org/package=readxl

Wickham, H., François, R., Henry, L., Müller, K., & Vaughan, D. (2023). *dplyr: A Grammar of Data Manipulation*. https://cran.r-project.org/package=dplyr

Wickham, H., Vaughan, D., & Girlich, M. (2023). *tidyr: Tidy Messy Data*. https://cran.r-project.org/package=tidyr

Wu, A. B., Li, H. P., Zhao, C. S., & Liao, Y. C. (2005). Comparative pathogenicity of

Fusarium graminearum isolates from China revealed by wheat coleoptile and floret inoculations. *Mycopathologia*, *160*(1), 75–83. https://doi.org/10.1007/s11046-005-1153-4

Wu, B., & Cox, M. P. (2021). Comparative genomics reveals a core gene toolbox for lifestyle transitions in Hypocreales fungi. *Environmental Microbiology*, *23*(6), 3251–3264. https://doi.org/10.1111/1462-2920.15554

Xu, X. M., Parry, D. W., Nicholson, P., Thomsett, M. A., Simpson, D., Edwards, S. G., Cooke, B. M., Doohan, F. M., Brennan, J. M., Moretti, A., Tocco, G., Mule, G., Hornok, L., Giczey, G., & Tatnell, J. (2005). Predominance and association of pathogenic fungi causing Fusarium ear blightin wheat in four European countries. *European Journal of Plant Pathology*, *112*(2), 143–154. https://doi.org/10.1007/s10658-005-2446-7

Zhan, J., Linde, C. C., Jürgens, T., Merz, U., Steinebrunner, F., & McDonald, B. A. (2005). Variation for neutral markers is correlated with variation for quantitative traits in the plant pathogenic fungus Mycosphaerella graminicola. *Molecular Ecology*, *14*(9), 2683–2693. https://doi.org/10.1111/j.1365-294X.2005.02638.x

Zhan, J., Pettway, R. E., & McDonald, B. A. (2003). The global genetic structure of the wheat pathogen Mycosphaerella graminicola is characterized by high nuclear diversity, low mitochondrial diversity, regular recombination, and gene flow. *Fungal Genetics and Biology*, *38*(3), 286–297. https://doi.org/10.1016/S1087-1845(02)00538-8

Zhang, Y., Chen, C., Mai, Z., Lin, J., Nie, L., Maharachchikumbura, S. S. N., You, C., Xiang, M., Hyde, K. D., & Manawasinghe, I. S. (2022). Co-infection of Fusarium aglaonematis sp. nov. and Fusarium elaeidis Causing Stem Rot in Aglaonema modestum in China. *Frontiers in Microbiology*, *13*(June), 1–14. https://doi.org/10.3389/fmicb.2022.930790

Figures

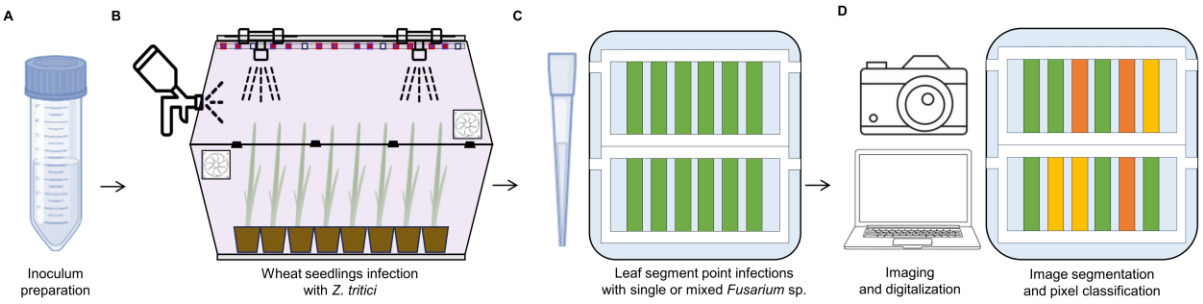

Figure 1. Overview of the phenotyping pipeline.

A 11-days-old *Z. tritici* (an hemibiotroph) culture was scratched from YMS plates, resuspended in TWEEN 0.01% (A) and sprayed in a closed environment (named as The Hive) where plants have kept until the appropriate stage (B). After 3 days, leaf fragments are harvested, mounted on agar plates and infected with a spore suspension of *Fusarium* spp. (a necrotroph) (C). After 4-7 dpi of incubation, pictures of the disease symptoms were taken with a Nikon camera. The pictures were analyzed with bash code throughout python scrIpts and the results were analyzed with R (D).

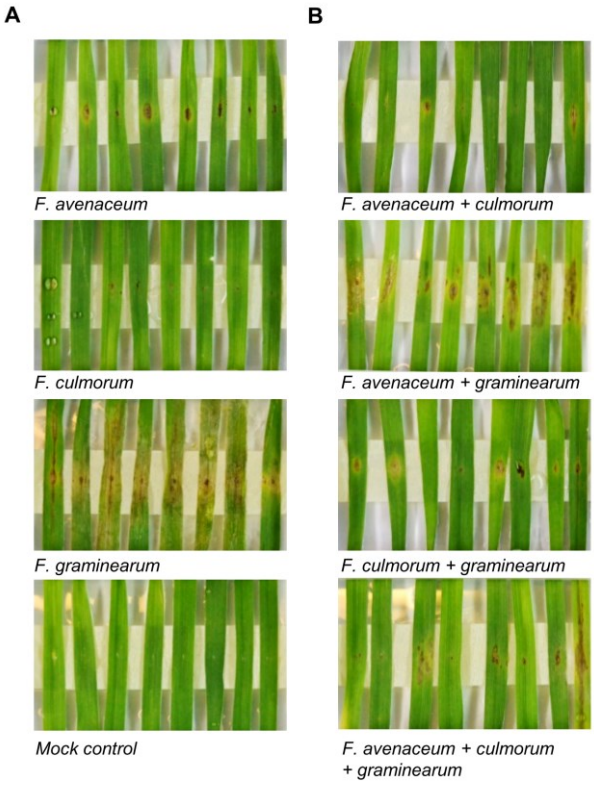

Figure 2. Phenotyping of Fusarium coinfections.

The cultivar Fielder was inoculated with *F. avenaceum*, *F. culmorum* and *F. graminearum* isolates from Sweden. Pictures were taken at 8 dpi. We perform two independent experiments with 8 biological replicates per treatment. We show representative pictures of one of the experiments.

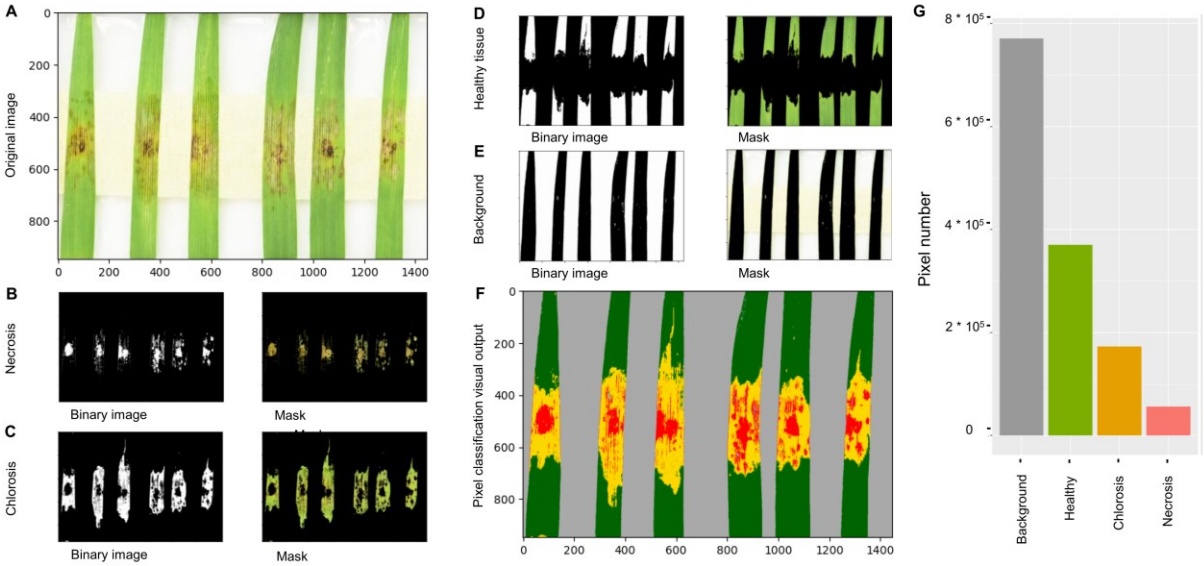

Figure 3. Steps for image analysis throughout quantification of Fusarium symptoms. A Naïve Bayes algorithm use a training set of pixels collected with the free software ImageJ to develops a probability function with the aim of classify all picture pixels in each of the predefined classes (necrosis, chlorosis, healthy tissue, or background). The result can be visualized in a binary image that is used to create a mask. All masks can be overlapped in a final image where is counted the number of pixels in each class, allowing the quantification of the disease symptoms.

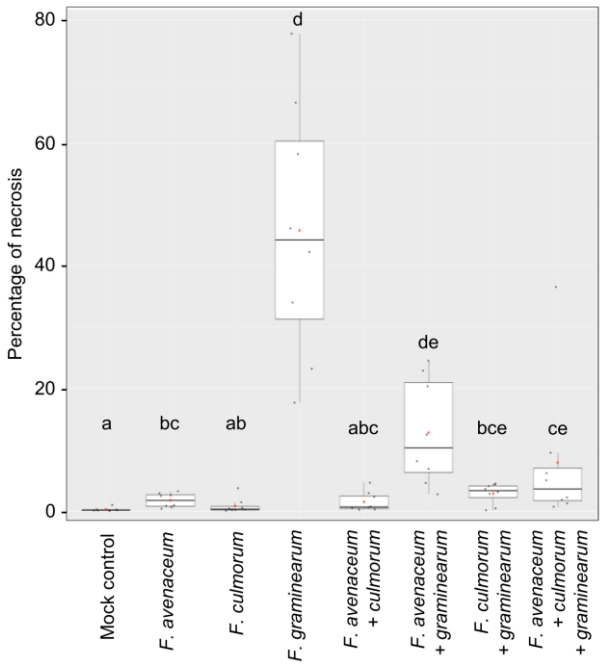

Figure 4. Symptom disease severity quantification through Naïve Bayes algorithm.
Pictures from Figure 2 were analyzed by the set up shown in Figure 3. The number of pixels classified as “Necrosis” was divided by the number of pixels calculated in the different groups of leaf pixels (“necrosis”, “chlorosis” and “healthy tissue”). The letters a-e refer to two groups of treatments that present differences statistically significative (two-way robust ANOVA: $p < 0.05$)

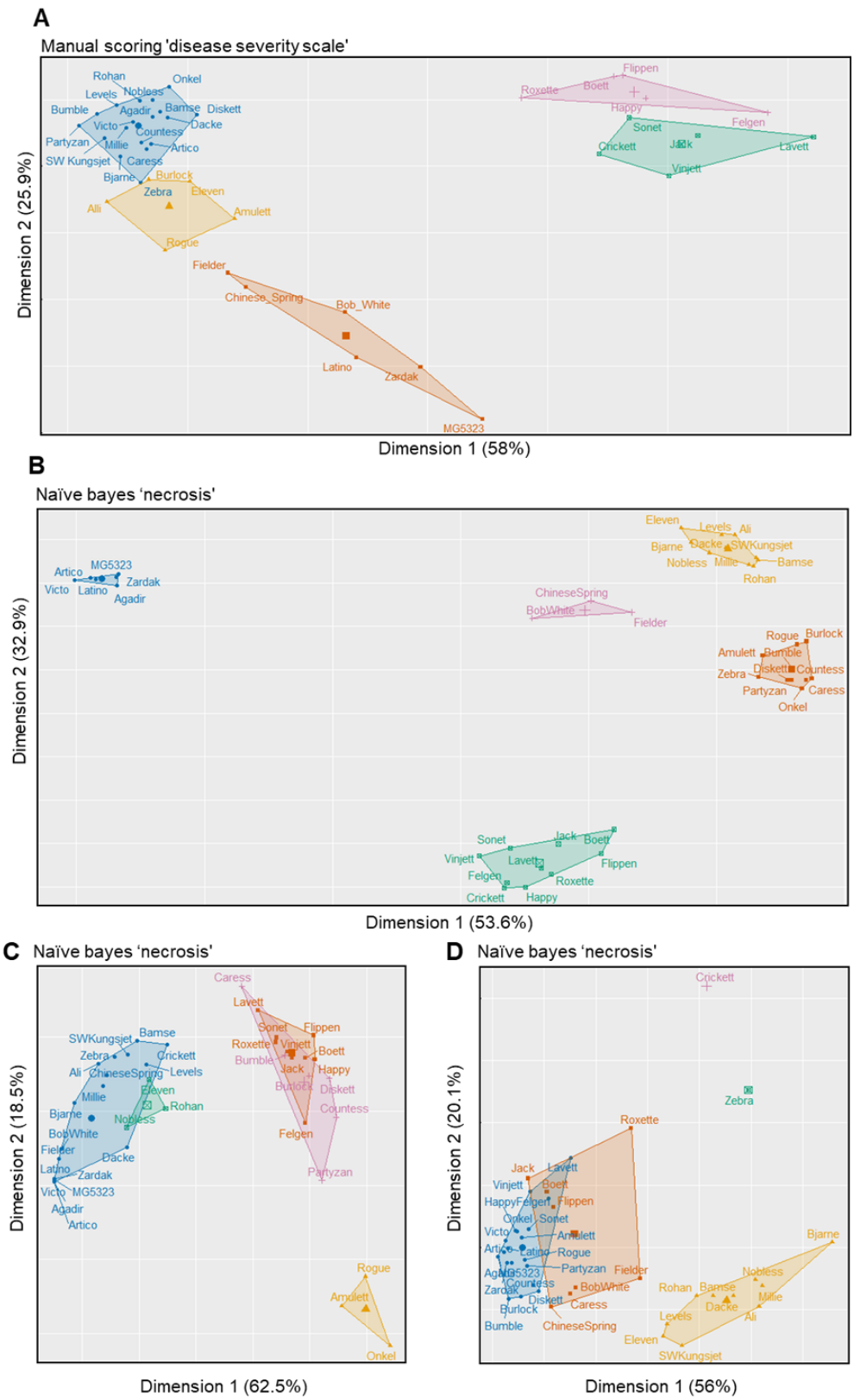

Figure 5. Cluster analysis of wheat cultivars infected with *F. avenaceum*, *F. culmorum*, *F. graminearum* alone or in combination.

The Agglomerative nesting (AGNES) algorithm was applied to the distance matrix of the mean value of the PCA coordinates of each sample to develop the dendrogram. The defined number of clusters is 5 (k = 5).

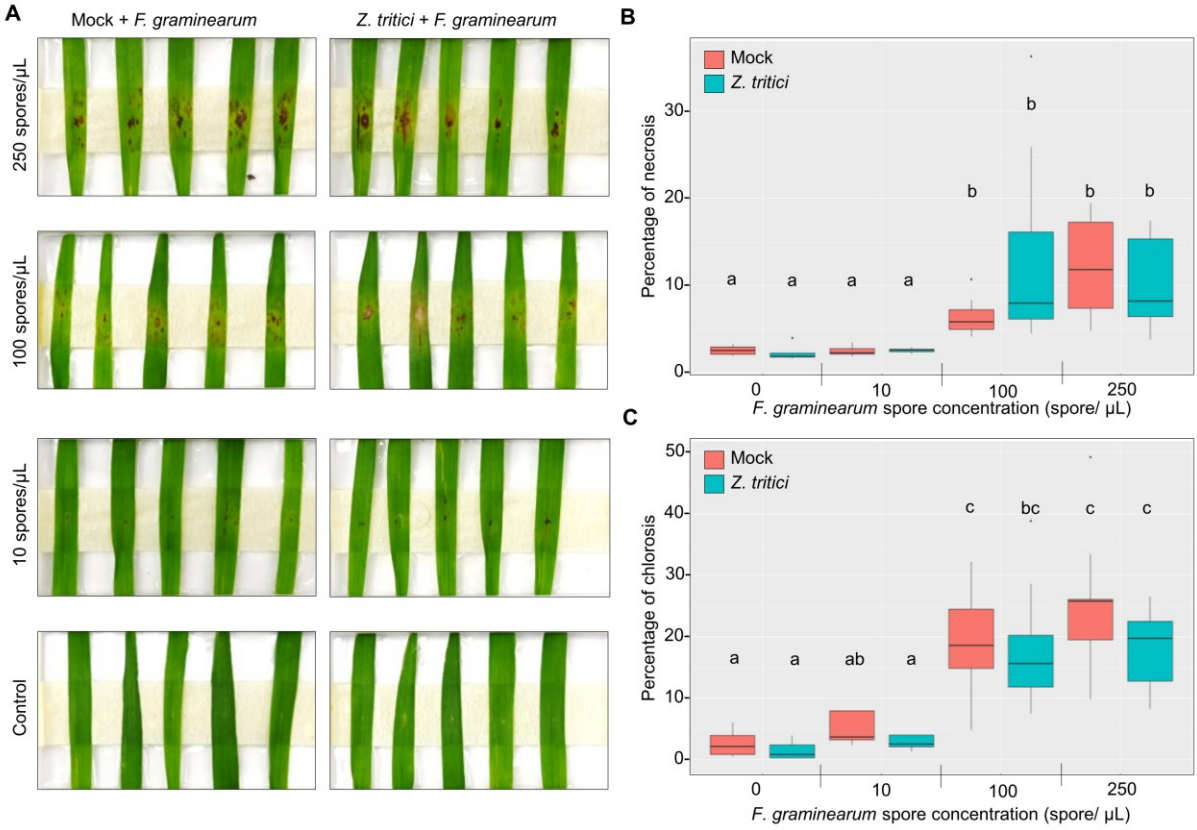

Figure 6. Quantification of the disease symptoms of *F. graminearum* at different spore concentrations in coinfections assays with *Z. tritici*.

(A) Pictures from one experiment with 5 biological replicates were analyzed with our setup at 5 dpi. The symptom quantification was obtained dividing the number of pixels counted in the class necrosis (B) or chlorosis (C) between the sum of the number of pixels in necrosis, chlorosis and healthy tissue classes. The pink color indicates mock treatment and blue color indicates plants coinfected with Z. tritici. The letters a-b refer to two groups of treatments that present differences statistically significative (two-way robust ANOVA: $p < 0.05$)

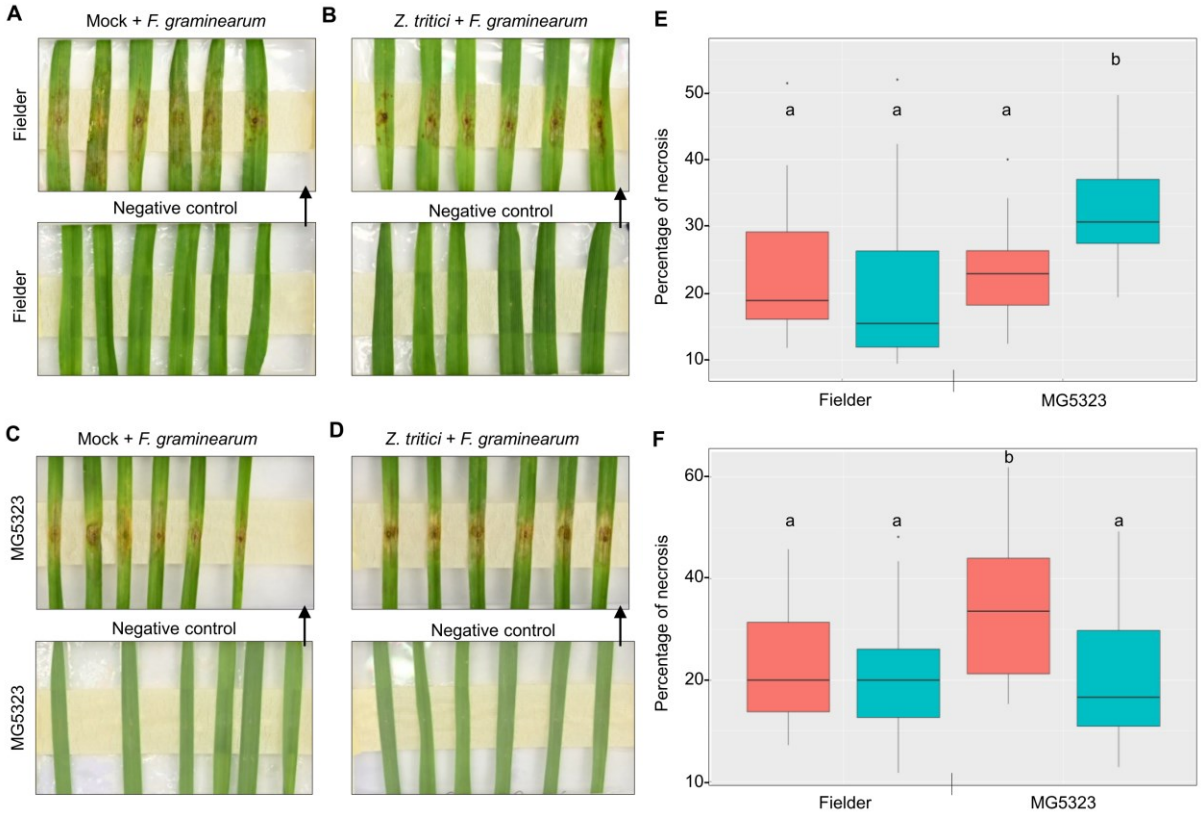

Figure 7. Quantification of the disease symptoms of *F. graminearum* in coinfections assays with *Z. tritici*.

(A) Pictures from two experiments with 6 biological replicates were analyzed with our setup. We show characteristic pictures of one experiment. The symptom quantification was obtained dividing the number of pixels counted in the class necrosis (B) or chlorosis (C) between the sum of the number of pixels in necrosis, chlorosis, and healthy tissue classes. The pink color indicates mock treatment and blue color indicates plants coinfected with *Z. tritici*. The letters a-b refer to two groups of treatments that present differences statistically significative (two-way robust ANOVA: $p < 0.05$)